Dynamical Climatology

An investigation of the Gates asynchronous coupling strategy using a simple energy-balance model.

by

D.L. Roberts

DCTN 64

March 1988

Meteorological Office (Met. O. 20)
London Road
Bracknell
Berkshire RG12 2SZ

DYNAMICAL CLIMATOLOGY TECHNICAL NOTE NO. 64

AN INVESTIGATION OF THE GATES ASYNCHRONOUS COUPLING STRATEGY USING A SIMPLE ENERGY-BALANCE MODEL

by

D L Roberts

Met O 20 (Dynamical
Climatology Branch)
Meteorological Office
London Road
Bracknell
Berkshire RG12 2SZ U.K.

March 1988

NOTE: This paper has not been published. Permission to quote from it should be obtained from the Assistant Director of the above Meteorological Office branch.

LF/M020

An investigation of the Gates asynchronous coupling strategy using a simple energy-balance model

1. Introduction

One of the most interesting types of experiment which can be performed with coupled general circulation models (GCMs) of the ocean and atmosphere is the attempted determination of the equilibrium response of the model climate system to some prescribed change in the background conditions, e.g. a rise in the atmospheric concentration of carbon dioxide. It has been realised for some time that to carry out such experiments in the natural way (referred to as synchronous coupling), in which the models run simultaneously and exchange information at frequent intervals, is not practicable with present computing resources. This is a consequence of the disparities between the various timescales involved: the atmospheric model requires far more computer time per simulated year than the oceanic model, while the oceanic model needs a much longer simulated time to attain equilibrium than the atmospheric model.

To overcome this difficulty, a number of approaches, collectively known as asynchronous coupling strategies, have been used or suggested. The essential feature of these is that the atmospheric model is run for short periods at intervals throughout the experiment, and its output time-averaged to provide the boundary conditions used to force the oceanic model between these periods. In some versions the oceanic model continues

to run while the atmospheric model is active, in others the models alternate. A valuable discussion of some of the different possibilities has been given by Schlesinger (1979).

However, asynchronous coupling can have undesirable side-effects. For instance, it may severely retard the convergence of the model climate system so that many more years must be simulated before equilibrium is reached. Asynchronous coupling can also cause instability, as in a case mentioned by Manabe et al (1979). Therefore one must assess the characteristics of a particular strategy very carefully before deciding to use it in a large-scale experiment for the first time.

The purpose of this note is to investigate the properties of a coupling strategy proposed by W L Gates (see Schlesinger 1979), shown schematically in Figure 1. In this strategy, the atmospheric and oceanic models are integrated synchronously for one year (this will be referred to as the synchronous phase), the oceanic model is then run by itself for a period of M years (the asynchronous phase), after which the models are recoupled and the cycle repeated. This is an example of what is sometimes termed periodically-synchronous coupling. The atmospheric data that provide the surface boundary conditions for the oceanic model during an asynchronous phase are taken from a library of 12 sets of the relevant physical quantities at the appropriate grid-points, each number being an average value for a month in the preceding synchronous phase. For example, the average surface air temperature field for August in a given synchronous phase is experienced by the ocean during every day of the M Augusts in the following asynchronous phase. (There is no magic about the number 12;

averaging over periods of a month is just a compromise between smoothing out synoptic fluctuations and retaining a fair description of the march of the seasons).

Gates' strategy has been selected for attention because it has some appealing features. For instance, it is fairly well adapted for use in experiments where the annual climatic cycle is simulated, unlike some earlier coupling strategies (see Schlesinger 1979) which are only suitable for experiments with no seasonal cycle. This is an important advantage, since the credibility of experiments with an annual mean insolation is rather low. Also, intuition suggests that a strategy with regular periods of synchronous running may be preferable to one in which the models never interact directly.

The present investigation was inspired and strongly influenced by the work of Dickinson (1981). While this note is intended to be self-contained, it is nevertheless true that a fuller picture will be obtained if it is read in conjunction with Dickinson's paper. His approach was to isolate the effects of a given coupling strategy by applying it to an extremely simple energy-balance model of the global climate. This consists of 3 thermal reservoirs representing the atmosphere, the ocean mixed layer and the intermediate water of the ocean, together with a crude representation of the energy transfers between them. The reservoirs are often referred to colloquially as 'boxes', and calling the model a 'box model' helps to distinguish it from the far more sophisticated energy-balance models (such as those reviewed by North et al, 1981) that are intended to simulate certain aspects of climatic change realistically.

It is important to understand the philosophy of this approach. The box model is a very simplified representation of only the most basic of the energy exchanges that occur in a coupled GCM system. It also fails to possess some important properties common to coupled GCMs and the real climate system, such as nonlinearity and noisiness. Therefore there is no guarantee that a coupling strategy which performs well in the context of the box model can successfully be applied to GCMs. However, a strategy that manifests problems when tried on the box model is most unlikely to be a satisfactory way of coupling GCMs. In other words, we have a convenient and cheap (though fallible) test for defective coupling strategies. There is also a positive aspect in that the simplicity of the box model makes it easier to perceive why some strategies fail, thus helping us to design better ones.

Two respects in which the present study differs from that of Dickinson (1981) should be noted. He discussed a slightly different coupling strategy, in which the atmospheric model is run to a statistically steady state with the ocean surface conditions prescribed, followed by a run of the ocean model for a fixed time interval with boundary conditions provided by the preceding atmospheric phase, and so on. This scheme is inferior to the Gates strategy and unsuitable for experiments which include the seasonal cycle. Consequently, Dickinson only considered the case of a constant (perturbation) forcing; in the present work an attempt is made to explore the possible effects of asynchronous coupling on the simulation of the seasonal cycle.

The problems associated with the choice of an asynchronous coupling strategy have also been studied in a recent pair of papers by Schneider and Harvey (1986) and Harvey (1986). The authors followed the same general approach as Dickinson (1981), but the energy-balance models they used are more complicated, e.g. the various contributions to the atmosphere-ocean heat flux are treated individually. Schneider and Harvey (1986) dealt with a globally-averaged annual mean model, while Harvey (1986) went on to consider a seasonally-varying model in which the globe is subdivided into boxes representing the land and sea in both the Northern and Southern Hemispheres. These papers cover a variety of coupling techniques and deserve a fuller discussion than can be given here; however it is important to note that Harvey (1986) concluded that some type of periodically-synchronous strategy is highly desirable.

The rest of this note is organised in the following way. The next section describes the box model that was used. Section 3 deals with experiments in which the model is forced by a constant perturbation heat flux; these resemble Dickinson's work, apart from the use of a different coupling strategy. Further insight into the results is provided by analysis presented in section 4, which supplements and extends Dickinson's treatment. Section 5 describes experiments in which the perturbation heat flux is sinusoidal, representing the seasonal cycle. Lastly, the main findings are reviewed in section 6.

2. The model

We consider the same system as Dickinson (1981), namely three ordinary differential equations that express (very crudely) the heat balances of the atmosphere, ocean mixed layer, and ocean intermediate water (subscripts a, m and o respectively):

$$C_a \frac{dT_a}{dt} + \lambda_{am}(T_a - T_m) + \lambda T_a = Q(t), \tag{2.1}$$

$$C_m \frac{dT_m}{dt} + \lambda_{am}(T_m - T_a) + \lambda_{mo}(T_m - T_o) = 0, \tag{2.2}$$

$$C_o \frac{dT_o}{dt} + \lambda_{mo}(T_o - T_m) = 0. \tag{2.3}$$

These are perturbation equations, in which the temperatures T_a, T_m, T_o and the heat flux $Q(t)$ are deviations from some notional equilibrium state. The constants C_a, C_m and C_o are the heat capacities of the boxes; λ_{am} and λ_{mo} are energy exchange coefficients between adjacent boxes; and the term λT_a represents the loss of energy to outer space due to long-wave radiation.

A list of the various assumptions and over-simplifications inherent in these equations would be quite long, and not particularly useful in view of the application we have in mind (see the introduction). However, it should be stressed that equations (2.1)-(2.3) are linear and thus qualitatively different from both the real climate system and coupled GCMs.

The set of all 3 equations will be referred to as the 3 box model. If we decouple the intermediate water by setting λ_{mo} to zero, the resulting pair of equations: (2.1) and

$$C_m \frac{dT_m}{dt} + \lambda_{am}(T_m - T_a) = 0 \quad , \qquad (2.4)$$

constitutes the 2 box model.

The parameters C_a, C_m, C_o, λ, λ_{am} and λ_{mo} were assigned the same values as those adopted by Dickinson (1981), except where otherwise noted. Thus (note that the model is for unit ocean surface area and time is measured in years):

$$\begin{aligned}
C_a &= 0{\cdot}45 \quad W m^{-2} \text{year} K^{-1}, \\
C_m &= 10 \quad W m^{-2} \text{year} K^{-1}, \\
C_o &= 100 \quad W m^{-2} \text{year} K^{-1}, \\
\lambda &= 2{\cdot}4 \quad W m^{-2} K^{-1}, \\
\lambda_{am} &= 45 \quad W m^{-2} K^{-1}, \\
\lambda_{mo} &= 2 \quad W m^{-2} K^{-1}.
\end{aligned}$$

These values give plausible timescales for heat exchange between the boxes - indeed it was mainly on this basis that the value of λ_{mo} was chosen (Dickinson, 1981).

Two kinds of experiment were performed. In the first, the perturbation forcing was a constant: $Q(t) = Q_o$ (corresponding, for example, to increased atmospheric heating due to a step-function increase in CO_2 concentration). In the second, the forcing was taken to be

sinusoidal, representing an idealised annual cycle:

$$Q(t) = Q_1 \cos(2\pi t) . \qquad (2.5)$$

There would be little point in examining a linear combination of these cases, because of the linearity of equations (2.1)-(2.3).

The equations were solved numerically using a Runge-Kutta method which is fourth-order accurate, i.e. the truncation error of the finite differencing is $O((\Delta t)^5)$. A timestep of half a day (Δt = 1/720) was used during synchronous phases; during asynchronous phases the timestep was $2^1/_2$ days. The calculations were performed in double precision arithmetic to avoid the danger of significant round-off error. Tests of the numerical accuracy were made: the 2 box model equations were solved analytically and the results agreed with the (synchronous) numerical solution to 5 significant figures. One long run of the 3 box model with asynchronous coupling was repeated with a timestep of only 1.25 days in the asynchronous phase, and the two sets of results were indistinguishable.

All experiments were started from zero initial conditions, i.e. the notional unperturbed state. With constant forcing the equilibrium response should be

$$T_a = T_m = T_o = \frac{Q_o}{\lambda} . \qquad (2.6)$$

To investigate the effects of the Gates coupling strategy described in the previous section, we treat equation (2.1) as an atmospheric GCM, while equations (2.2) and (if present) (2.3) play the part of the oceanic GCM. Thus during an asynchronous phase, equation (2.1) is decoupled from the system and equation (2.2) is replaced by:

$$C_m \frac{dT_m}{dt} + \lambda_{mo}(T_m - T_o) = \lambda_{am}(F(t) - rT_m), \qquad (2.7)$$

where r is Dickinson's implicitness parameter (see below) and

$$F(t) \equiv ALIB(t) - (1-r)MLIB(t). \qquad (2.8)$$

Instead of the 'true' atmosphere/mixed layer heat flux $\lambda_{am}(T_a - T_m)$, we now have a forcing term involving the 'libraries' ALIB and MLIB, which contain the average values of T_a and T_m for the months in the preceding synchronous phase.

The significance of the parameter r may be understood by considering two extreme cases. If $r = 0$ the heat flux forcing the ocean is always the same as in the corresponding month during the previous synchronous phase, regardless of how ocean conditions have evolved since then; Dickinson (1981) termed this explicit coupling. If $r=1$ the current mixed layer temperature, together with the air temperature from the appropriate month of the synchronous phase, is used to compute the heat flux. This is referred to as implicit coupling. Choosing an intermediate value of r (semi-implicit coupling) results in a linear combination of these methods.

It should also be mentioned that although r has been introduced here as a single number in the context of a globally-averaged model, in the case of a coupled system of GCMs the natural generalisation is to regard r as a function of position. Indeed, Dickinson (1981) pointed out that there may well be advantages to be gained by choosing a non-uniform implicitness parameter, because of geographical variations in the rate of atmosphere-ocean coupling. An exploration of these possibilities clearly demands a more complicated model than the present one (e.g. a zonal-mean energy-balance model), and will not be attempted here. Nevertheless it should be borne in mind throughout the following sections that in practice one may wish to use a small range of values of r instead of a single number.

3. Experiments in which the perturbation forcing is constant

The first part of this section deals with some results from numerical integrations of the 2 box model. Results for the 3 box model will be presented subsequently.

In the 2 box case, with the large thermal capacity of the intermediate water absent, the system should converge to the equilibrium state given by (2.6) fairly quickly. The synchronous solution indeed does so: after 30 years T_a and T_m reach about 99.9% of their equilibrium values. (Remember that for present purposes the synchronous solution may be regarded as essentially exact, as was noted in section 2).

In the asynchronous experiments, the coupling cycle used (except where otherwise stated) was 9 asynchronous years between every synchronous year. A selection of values of the implicitness parameter, ranging between r = 0.05 and 1.0, were tried. One of the most interesting aspects of the results is the dependence of the rate of convergence on r . Following Dickinson (1981), we define a convergence ratio R by (in the case of the standard coupling cycle)

$$R(t) = \frac{T_m(t) - T_m(t-10)}{T_m(t-10) - T_m(t-20)} \quad . \qquad (3.1)$$

This expression will normally be evaluated during a synchronous phase. So R is the ratio of the difference between the current mixed layer temperature and its value at the same time of year 10 years ago, in the previous synchronous phase, to the same difference lagged by 10 years. Thus if R

is small in magnitude, the mixed layer temperature is converging rapidly; if $|\mathcal{R}| > 1$ consistently we have instability, and if $-1 < \mathcal{R} < 0$ there is oscillating convergence. It turns out that the dependence of $\mathcal{R}$ on the time of year is so weak that we can completely ignore it. This applies even to the experiments with seasonally-varying forcing which are discussed in section 5. In most cases it is also true that $\mathcal{R}$ does not vary significantly during the entire course of the integration.

The rapidly-convergent synchronous solution has a convergence ratio of about 0.11. Compare this with the convergence ratios of the various asynchronous solutions, which are plotted against the implicitness parameter in Figure 2. Evidently most of the asynchronous solutions converge much more slowly than the synchronous solution. We can also see that the effect of varying r is highly nonlinear. (Note: the value of $\mathcal{R}$ at $r = 0.055$ shown in Figure 2 is somewhat less accurate than the rest of the data, because in this case $\mathcal{R}$ oscillates in time with diminishing amplitude, converging to about 0.35. The corresponding values of T_m do not oscillate, though).

Now Dickinson (1981) studied the 2 box model analytically, and amongst other things discussed the dependence of $\mathcal{R}$ on r. Examining Figure 2 of his paper, one finds that if the interval between synchronous phases is long enough to be useful in practice, the analysis predicts the same kind of behaviour that we have found: very slow convergence over most of the range, with a sharp improvement near a small (but non-zero) value of r. At smaller values of r the convergence is oscillatory, and when r is decreased still further the oscillations become unstable. In

particular, the explicit coupling case ($r = 0$) is predicted to be unstable. The analysis further predicts that the critical value of r, at which R is equal to the synchronous convergence ratio and the changeover from monotonic to oscillating convergence occurs, is $\lambda/(\lambda + \lambda_{am})$; notice that this is independent of the lengths of the synchronous and asynchronous phases. With the parameter values we have used, this critical number is about 0.0506 (just below the lowest value of r seen in Figure 2).

Although Gates' coupling strategy is somewhat different from the one investigated by Dickinson (1981), as explained in section 1, it is reasonable that the dependence of R on r should be similar in the two cases. For the role played by r in the heat transfer formulation is identical. This suggests that the same type of behaviour may be encountered when the semi-implicit heat transfer idea is used with other coupling strategies, provided they are not radically different from the Gates strategy.

As pointed out by Dickinson, these results indicate that one ought to be very careful in choosing r, since there is only a small range of favourable values between the twin dangers of extremely slow convergence on the one hand, and unphysical oscillations on the other. However, Dickinson also made it clear that the slower convergence of the synchronous solution expected when the deeper water of the ocean is taken into account may well affect these conclusions (although he was unable to extend his analytical treatment to the 3 box model). We therefore move on to consider the 3 box case.

Figure 3 shows the development in time of the mixed layer temperature for the synchronous solution (the top curve) and for asynchronous solutions with various values of r : working upwards from the lowest curve they are r = 1.0, 0.75, 0.5, 0.25, 0.2, 0.15, 0.1 and 0.05. Note that T_m has been normalised by its equilibrium value (eq. (2.6)). Figure 4 displays the corresponding curves for T_o . It is interesting that T_o evolves smoothly, whereas (except in the nearly explicit cases) T_m changes far more during a synchronous year than in the nine asynchronous years that follow. A heuristic explanation of this will now be given.

First, it is important to note that

$$\lambda_{am} \gg \lambda, \lambda_{mo} , \tag{3.2}$$

i.e. the coupling between the atmosphere and mixed layer is strong compared with the radiative damping and the mixed layer/deeper water coupling. The effect of (3.2), combined with the much greater thermal inertia of the deeper water, means that T_a and T_m stay fairly close to each other during a synchronous phase. Thus T_m will not be far below T_a at the end of a synchronous phase. During the subsequent asynchronous phase, the ocean is forced by the term on the right hand side of (2.7), which is our attempt to estimate what the atmosphere/mixed layer heat flux should be. If $r = 1$, so that this heat flux is based on the current value of T_m , and the appropriate value of T_a stored during the previous synchronous phase, T_m will clearly be restrained from rising above this value of T_a . Since T_m was not far below T_a to begin with, it follows that T_m cannot increase

very much, however long the asynchronous phase lasts. Thus we obtain the staircase-like behaviour of T_m shown in Figure 3. (Of course, this argument does not explain why r must be made so much less than 1 before the staircase phenomenon dies out. However, that question is covered, in effect, by the more rigorous discussion in the next section.)

Pursuing our heuristic argument, consider next how T_o will respond to the staircase-like evolution of T_m. For simplicity, imagine that $T_m(t)$ is a step function:

$$T_m(t) = \begin{cases} 0 , & t \leq 0 \\ \tilde{T}_m , & t > 0 \end{cases} , \qquad (3.3)$$

where $\tilde{T}_m$ is a constant. Then (2.3) becomes, for $t > 0$,

$$C_o \frac{dT_o}{dt} + \lambda_{mo} T_o = \lambda_{mo} \tilde{T}_m , \qquad (3.4)$$

and the solution of this with $T_o(0) = 0$ (for example) is

$$T_o(t) = \tilde{T}_m \left(1 - \exp\left[-\frac{\lambda_{mo}}{C_o} t\right]\right) . \qquad (3.5)$$

Thus T_o reacts to a step function increase in T_m on a timescale of order C_o / λ_{mo} = 50 years. This is sufficiently long compared with the length of the coupling cycle that T_o is unable to follow the sharp changes in T_m, and so evolves smoothly.

Returning to Figures 3 and 4, one is again struck by the nonlinear effect of varying r, noted earlier in the context of the 2 box model. Clearly, when $r = 0.05$ the asynchronous solution follows the synchronous solution rather well. In theory, then, such 'almost-explicit' coupling has much to commend it.

Another noteworthy point is that, if convergence time is defined as the time taken for T_m to attain 95% of its equilibrium value, then the ratio of the convergence time of the fully implicit asynchronous solution to the convergence time of the synchronous solution is only about 1.4 for the 3 box model, compared with roughly 9.5 in the 2 box case. This supports Dickinson's suggestion that the retarding effect of fully implicit coupling may be much less damaging when the synchronous solution itself converges slowly.

The details of these results clearly depend, to some extent, on the values assumed for the parameters that appear in equations (2.1)-(2.3). Further experiments have therefore been carried out to investigate the effects of varying some of the parameters. These will not be reported at length here, but to illustrate the possibilities the results of two such experiments will be given. Because Dickinson (1981) emphasized the particular uncertainty attached to the value of λ_{mo} (2 Wm^{-2} K^{-1} in the run just discussed), we consider the impact of changing it while leaving all other features of the standard experiment unaltered.

Figures 5 and 6 show the evolution of T_m and T_o if $\lambda_{mo} = 8 (Wm^{-2}K^{-1})$ (According to Dickinson this is near the upper limit of the range of credible values for λ_{mo} .) Comparing Figure 5 with Figure 3, we see that the much stronger coupling between the mixed layer and the intermediate water slows down the initial response of T_m to the perturbation forcing. The other side of the coin, of course, is that T_o now rises more quickly (Figure 6 cf Figure 4), and in the long run this results in faster convergence to equilibrium. If we compare the extent to which fully implicit asynchronous coupling retards convergence in the two cases, it is apparent that the damage is relatively worse when $\lambda_{mo} = 8$ — another example of the principle that fully implicit coupling does less harm when the synchronous solution converges more slowly.

The results of an experiment in which λ_{mo} was 0.5 ($Wm^{-2}K^{-1}$) are shown in Figures 7 and 8. With this weaker coupling, the temperature of the mixed layer is able to reach a higher level before an approximate balance is set up between the incoming heat flux from the atmosphere and the outgoing flux to the intermediate water. However, further progress is very slow once this balance has been established. As one would expect, this mitigates the effects of fully implicit coupling.

Finally, it is worth noting the outcome of using explicit coupling. Figures 9 and 10 display the time development of T_m and T_o in an experiment in which $r = 0$ and $\lambda_{mo} = 2$, with the corresponding synchronous solutions given for comparison. Oscillations of large amplitude in T_m occur, because the atmosphere/ocean heat flux experiences no feedback from the mixed layer temperature during

asynchronous phases. Although the large thermal inertia of the intermediate water ensures that the oscillations are damped, this type of behaviour is undesirable for practical purposes, because of the nonlinear feedback processes which are present in GCMs.

4. Analysis of the constant forcing case

The object of this section is to illuminate the role of the implicitness parameter r by analytical methods. Though Dickinson's (1981) analysis is drawn upon, the work to be presented includes a substantial amount of new material. In particular, it will be shown how the adoption of a slightly different approach enables the 3 box case to be treated.

Following Dickinson, we begin by noting that during any synchronous phase, equation (2.1) (with $Q(t) = Q_o$) has the approximate solution

$$T_a(t) = \frac{Q_o + \lambda_{am} T_m(t)}{\lambda + \lambda_{am}} \cdot \left(1 - e^{-\alpha(t-t_o)}\right) + T_a(t_o) e^{-\alpha(t-t_o)}, \qquad (4.1)$$

where t_o (an integer) is the time at which the phase began, and

$$\alpha \equiv \frac{\lambda + \lambda_{am}}{C_a} \simeq 100 \ (yr^{-1}) \ . \qquad (4.2)$$

This statement applies equally well to both 2 and 3 box cases, of course. Because α is large, T_a rapidly adjusts to dynamic equilibrium with the mixed layer temperature during the first fortnight of a synchronous phase.

From then on, it is a very good approximation to write

$$T_a = \frac{Q_o + \lambda_{am} T_m(t)}{\lambda + \lambda_{am}} \quad . \tag{4.3}$$

We now begin to depart from Dickinson's treatment. Let $\hat{T}_a(t)$ and $\hat{T}_m(t)$ be the 'library' functions which contain the average values of T_a and T_m for the months in the synchronous phase, used to force the mixed layer equation during the subsequent asynchronous phase. The formal definitions of these are:

$$\hat{T}_{a,m}(t) = 12 \int_{t' = t_1(t)}^{t_1 + \frac{1}{12}} T_{a,m}(t')\, dt' \quad , \tag{4.4}$$

where

$$t_1(t) = \frac{1}{12} \mathrm{Int.} \left\{ 12 (t - \mathrm{Int.}(t - t_o)) \right\} \quad , \tag{4.5}$$

$\mathrm{Int.}(x)$ being the integer part of x .

From (4.3), it is clear that for $t_1(t) \geqslant \frac{1}{12}$,

$$\hat{T}_a(t) = \frac{Q_o + \lambda_{am} \hat{T}_m(t)}{\lambda + \lambda_{am}} \quad . \tag{4.6}$$

Because (4.3) does not hold during the first fortnight of a synchronous phase, an error will be incurred if (4.6) is used for $t_1(t) < \frac{1}{12}$. This error can be shown to be closely approximated by $\frac{12}{\alpha}\left(T_a(0) - T_a(0)_{est}\right)$, where the subscript **est** indicates the value of $T_a(0)$ given by (4.3). Although this correction is not unimportant, it is small enough that for present purposes we can neglect it, and assume that (4.6) is valid throughout the year.

In the next asynchronous phase we have, from (2.7) and (2.8),

$$C_m \frac{dT_m}{dt} + \lambda_{mo}(T_m - T_o) = \lambda_{am}\left\{\hat{T}_a - (1-r)\hat{T}_m - rT_m\right\} . \qquad (4.7)$$

The aim now is to rewrite this equation in a form that brings out the significance of r . To this end, we introduce the equilibrium temperature T_e , given by (2.6), and also the critical value of the implicitness parameter (identified by Dickinson), r^* :

$$T_e = \frac{Q_o}{\lambda} , \qquad (4.8)$$

$$r^* = \frac{\lambda}{\lambda + \lambda_{am}} . \qquad (4.9)$$

Now (4.6) can be rearranged to give

$$\hat{T}_a - \hat{T}_m = \frac{\lambda}{\lambda_{am}}\left(T_e - \hat{T}_a\right) , \qquad (4.10)$$

so that (4.7) becomes

$$C_m \frac{dT_m}{dt} + \lambda_{mo}(T_m - T_o) = \lambda_{am}\left\{ r(\hat{T}_a - T_m) + \frac{\lambda}{\lambda_{am}}(1-r)(T_e - \hat{T}_a) \right\}. \qquad (4.11)$$

Since $$\lambda_{am} r - \lambda(1-r) = (\lambda + \lambda_{am})(r - r^*) \,, \qquad (4.12)$$

$$C_m \frac{dT_m}{dt} + \lambda_{mo}(T_m - T_o) = r\lambda_{am}(T_e - T_m) - (\lambda + \lambda_{am})(r - r^*)(T_e - \hat{T}_a). \qquad (4.13)$$

Using (4.6) again,

$$T_e - \hat{T}_a = \frac{\lambda_{am}}{\lambda + \lambda_{am}}(T_e - \hat{T}_m) \,, \qquad (4.14)$$

whence

$$C_m \frac{dT_m}{dt} + \lambda_{mo}(T_m - T_o) = r\lambda_{am}(T_e - T_m) - \lambda_{am}(r - r^*)(T_e - \hat{T}_m). \qquad (4.15)$$

This form of the asynchronous T_m equation is conceptually useful, because it contains no reference to the air temperature, and allows the effect of varying r to be readily identified. To appreciate the latter point, consider the two contributions into which the atmospheric forcing term has now been split. The first term on the right hand side of (4.15) encourages T_m to converge to its (correct) equilibrium value, T_e. The second term, which is constant except for changes at the end of every month, tends to retard convergence if $r > r^*$, or causes overshooting (and thus oscillatory convergence or instability) if $r < r^*$.

The optimal value of r is clearly r^*, since the second term then vanishes. Since $\lambda \ll \lambda_{am}$, r^* is much nearer zero than one. However, because it seems unlikely that we could know the exact value of r^* in the practical context of coupled GCMs, especially as there will be spatial variations (see section 2), it is interesting to ask how large $|r - r^*|$ can be made before convergence is seriously damaged. We choose to concentrate on the case $r > r^*$, since oscillations are undesirable even if they are convergent. Therefore put

$$r = r^* + \varepsilon, \tag{4.16}$$

and examine the ratio of the retarding term to the 'helpful' forcing term,

$$\rho_1 = \frac{\varepsilon (T_e - \hat{T}_m)}{(r^* + \varepsilon)(T_e - T_m)} . \tag{4.17}$$

If $r > r^*$, convergence should be monotonic, thus

$$\frac{T_e - \hat{T}_m}{T_e - T_m} > 1 . \tag{4.18}$$

Hence if ρ_1 is to be small, we require

$$\frac{\varepsilon}{r^* + \varepsilon} \ll 1 , \quad \text{i.e.} \quad \varepsilon \ll r^* . \tag{4.19}$$

Leaving aside for the moment the influence of the coupling to the deeper water, i.e. considering the 2 box model, it is clear from (4.19) that r cannot be made significantly larger than r^* without seriously slowing down the convergence of T_m. For instance, if r is only as much as $2r^*$ (about 0.1 with the standard parameter values), then $\rho_1 \geq \frac{1}{2}$. This conclusion agrees with the results of Dickinson's (1981) analysis and the numerical calculations of the present paper (e.g. Figure 2): see the discussion in section 3. However, we can now go somewhat further than Dickinson by making a quantitative assessment of how the picture alters if the deeper water is taken into account.

Consider the ratio of the retarding term to the one involving T_o :

$$\rho_2 = \frac{\lambda_{am}(r - r^*)(T_e - \hat{T}_m)}{\lambda_{mo}(T_m - T_o)} \quad . \tag{4.20}$$

If ρ_2 is small compared with unity, the synchronous solution converges so slowly (due to the retarding effect of the deeper water) that asynchronous coupling imposes little further penalty. On the other hand, if ρ_2 is fairly large (say ≥ 10) then the conclusions reached for the two box case carry over to the three box model.

As before, we assume that $r > r^*$ and convergence is thus monotonic. Then T_m and T_o always lie in the interval $[0, T_e]$, so that

$$|T_m - T_o| < T_e \quad . \tag{4.21}$$

Hence $$|\rho_2| > \frac{\lambda_{am}}{\lambda_{mo}}(r - r^*)\left(1 - \frac{\hat{T}_m}{T_e}\right) . \qquad (4.22)$$

With the standard values of the λ coefficients (section 2), $\frac{\lambda_{am}}{\lambda_{mo}} = 22{\cdot}5$, so that (4.22) suggests that the retardation due to asynchronous coupling is significant, in the fully implicit $(r = 1)$ case, until the mixed layer temperature has risen to at least 95% of its equilibrium value. Figures 3 and 4 would appear to confirm this; for instance after 200 years the fully implicit asynchronous solution for T_m lags behind the synchronous solution by approximately 70 years, whereas after 300 years the gap has widened to about a century. (In practice, this degree of retardation would probably be just about acceptable).

A final remark concerning (4.20) may be of interest. Because the initial response of the mixed layer is much more rapid than that of the deeper water, ρ_2 tends to decrease fairly quickly during the first three decades. Thus the retarding effect of asynchronous coupling is more important near the start of an experiment than it is later on. This suggests that it might be useful to vary the proportion of time spent in synchronous running, ω say, as a run proceeds; a reasonable plan would be to start with a relatively high value of ω and gradually reduce it subsequently. (This plan has already been proposed by Harvey (1986), for slightly different reasons). Some preliminary tests of this idea have been made: they appear to show a beneficial impact, but it is not yet clear whether much advantage can be gained.

5. Experiments in which the perturbation forcing is sinusoidal

In sections 3 and 4, much of the discussion was focused on the rates of convergence of various asynchronous solutions towards a known equilibrium state. When we come to consider the case of seasonal forcing, a new issue arises: is the asynchronous equilibrium state correct? This question, though of some importance, does not appear to have been addressed before.

The experiments to be described here are similar in most respects to those of section 3, unless otherwise stated, except that the perturbation heat flux is

$$Q(t) = Q_1 \cos(2\pi t) \quad . \tag{5.1}$$

Because the model is linear, the size of Q_1 is to some extent arbitrary. However the value chosen, $Q_1 = 100\,Wm^{-2}$, is of a realistic order of magnitude.

It turns out that the equilibrium response of T_a and T_m to the forcing (5.1) is almost the same in a 3 box model experiment as it is in the analogous 2 box model experiment. (This statement applies to both synchronous and asynchronous solutions.) The explanation for this is simply that the intermediate water box reacts too slowly to be significantly excited by oscillations with a period of one year (cf the response of T_o to a step function, in section 3). The following

discussion will therefore be restricted to the 3 box case alone. A further simplification will be made by confining attention to the fully implicit case $(r = 1)$.

Consider then the graphs of mixed layer temperature against time (in months) shown in Figure 11. The plain curve is the equilibrium annual cycle of the synchronous solution; it lags about 3 months behind the forcing flux (5.1), which is reasonable. The marked curve is the asynchronous solution during a synchronous phase, after equilibrium has been reached. Manifestly there is a small but systematic difference between them.

Before an attempt is made to explain this discrepancy, consider Figure 12, which shows the difference

$$\Delta T_m = T_m\big|_{sync} - T_m\big|_{async} , \qquad (5.2)$$

during an 11-year sequence (at equilibrium) which covers an entire asynchronous phase and the synchronous phases on either side. The synchronous solution has a period of one year, of course; it happens that after three years of the asynchronous phase, the asynchronous solution also repeats itself annually, to a very good approximation; so that ΔT_m does likewise. (Assuming that the effect of the intermediate water can be neglected, it is not difficult to prove that this occurs during every asynchronous phase, even before equilibrium has been established). Figure 12 also shows that ΔT_m decreases steadily during each synchronous phase,

this tendency for the asynchronous solution to approach the synchronous equilibrium cycle being cancelled out during the first year of the following asynchronous phase.

The reasons why the synchronous and asynchronous equilibria differ are not yet fully understood. However, two factors seem to be involved. The first is the representation, during asynchronous phases, of the annual cycle of forcing by only 12 values. This appears to be unsatisfactory, for in an experiment in which the forcing term $F(t)$ ((2.8)) was computed by linear interpolation between the libraries of monthly averages, an asynchronous equilibrium very close to the synchronous one was obtained. (The maximum of ΔT_m was approximately 4% of its value in the standard run - a negligible error).

Secondly, it is also relevant that at the beginning of each synchronous phase, T_m will in general be different from its value at the end of the previous synchronous phase, whereas T_a will perforce be unchanged. Thus the atmosphere must adjust to reacquire thermal balance with the ocean. This will be achieved within a fortnight (section 4), but nevertheless the average of T_a for the first month of the year will contain a significant input from temperatures that are out of balance. Consequently, there is liable to be some distortion of the behaviour of T_m during the first month of every year in the following asynchronous phase. This idea is supported by the results of a number of experiments in which the phase of the forcing was altered, i.e.

$$Q(t) = Q_1 \cos\{2\pi(t+\psi)\}, \qquad (5.3)$$

where ψ is fixed during a given experiment. It turns out that if ψ is chosen so that years commence at a time when the equilibrium synchronous solutions for T_a and T_m are equal, so that only a small initial readjustment by the atmosphere is required, the error in the asynchronous equilibrium cycle is an order of magnitude lower than if $\psi = 0$. It is also worth noting that in Figure 12, the peaks in ΔT_m during the asynchronous phase occur after the first month of each year.

At this point it is important to stand back from the details of these experiments, and assess their implications for the Gates strategy in the broader context of general circulation models. We have identified two unfortunate features of the Gates strategy: the inadequate representation of the seasonal cycle; and the use, during asynchronous phases, of conditions during the initial readjustment periods of the synchronous phases. It seems likely that these will continue to be weaknesses in the GCM context, though their consequences may well be more subtle. Since it is possible to remove these defects without sacrificing any of the desirable elements of the Gates strategy (see next section), it would be sensible to do so.

Finally, although this section has concentrated on the fully implicit case, the results of similar experiments with $r < 1$ deserve mentioning. If r is reduced, the error in the asynchronous equilibrium cycle

gradually decreases. At about $r = 0.2$ the error crosses zero and its size increases again; however the (equilibrium) error at $r = 0.1$ is an order of magnitude less than that obtained in the fully implicit case.

6. Conclusions

This note has examined the asynchronous coupling strategy due to Gates, by testing it on a simple energy-balance or 'box' model. Of course, there is a wide gulf between the box model and a coupled GCM, and it is dangerous to push the analogy between the systems too far. However, on the evidence presented here there is no reason to suppose that the Gates strategy, slightly modified as explained below, is unsuitable for serious use with GCMs.

Two unfavourable features of the strategy have been identified.

i. During asynchronous phases, the seasonal cycle in atmospheric quantities that force the ocean consists of 12 step-function changes.

ii. Conditions during the initial readjustment period of a synchronous phase are allowed to influence developments in the following asynchronous phase.

The possible effects of i. and ii. in a GCM context cannot be anticipated from the results of box model experiments. However, since neither feature is fundamental to the scheme, it is recommended that they be eliminated in the following ways. First, the data needed to drive the ocean during asynchronous phases should be obtained by interpolating in time between the monthly average values held in libraries. Secondly, synchronous phases should be longer than a year - at least 13 months - with the libraries of forcing data being formed during the final 12 months of the phase.

The part played by the implicitness parameter r has also been discussed. Although the strategy considered by Dickinson (1981) differs slightly from the Gates strategy, we have seen that his conclusions remain valid in the Gates case. The best choice of r is theoretically r^* (4.9), a number likely to lie between zero and 0.1 in practice. Unfortunately, it is necessary to estimate r^* more accurately than this in order to reap anything like the full benefit of the semi-implicit method. This is not easily done, but need not be dismissed as an impossible task; a feasible approach has been suggested by Dickinson. Until an estimate of r^* is available, the best option is fully implicit coupling, $r = 1$, because it is economical on computer storage without having significantly worse convergence properties than (for example) $r = \frac{1}{2}$.

Some questions remain to be answered. In particular, although we have concluded that synchronous phases should last more than a year, no attempt has been made to decide what their optimal duration is. This presupposes that ω, the fraction of a cycle occupied by the synchronous phase, is regarded as a given constant. There is also a possibility that it may be profitable to vary ω in the course of an experiment, as mentioned at the end of section 4. Any future work on this topic ought to address these issues.

7. Acknowledgment

I am grateful to Howard Cattle, William Ingram, John Mitchell, Peter Rowntree, and Clive Wilson, for their advice and encouragement at different stages of this work.

References

Dickinson, R.E. 1981 Convergence rate and stability of ocean-atmosphere coupling schemes with a zero-dimensional climate model. J. Atmos. Sci., 38, 2112-2120.

Harvey, L.D.D. 1986 Computational efficiency and accuracy of methods for asynchronously coupling atmosphere-ocean climate models. Part II. Testing with a seasonal cycle. J. Phys. Oceanogr., 16, 11-24.

Manabe, S., Bryan, K. and Spelman, M.J. 1979 A global ocean-atmosphere climate model with seasonal variation for future studies of climate sensitivity. Dyn. Atmos. Oceans, 3, 393-426.

North, G.R., Cahalan, R.F. and Coakley, J.A. 1981 Energy balance climate models. Rev. Geophys. Space Phys., 19, 91-121.

Schlesinger, M.E. 1979 Discussion of 'A global ocean-atmosphere climate model with seasonal variation for future studies of climate sensitivity'. Dyn. Atmos. Oceans, 3, 427-432.

Schneider, S.H. and Harvey, L.D.D. 1986 Computational efficiency and accuracy of methods for asynchronously coupling atmosphere-ocean climate models. Part I. Testing with a mean annual model. J. Phys. Oceanogr., 16, 3-10.

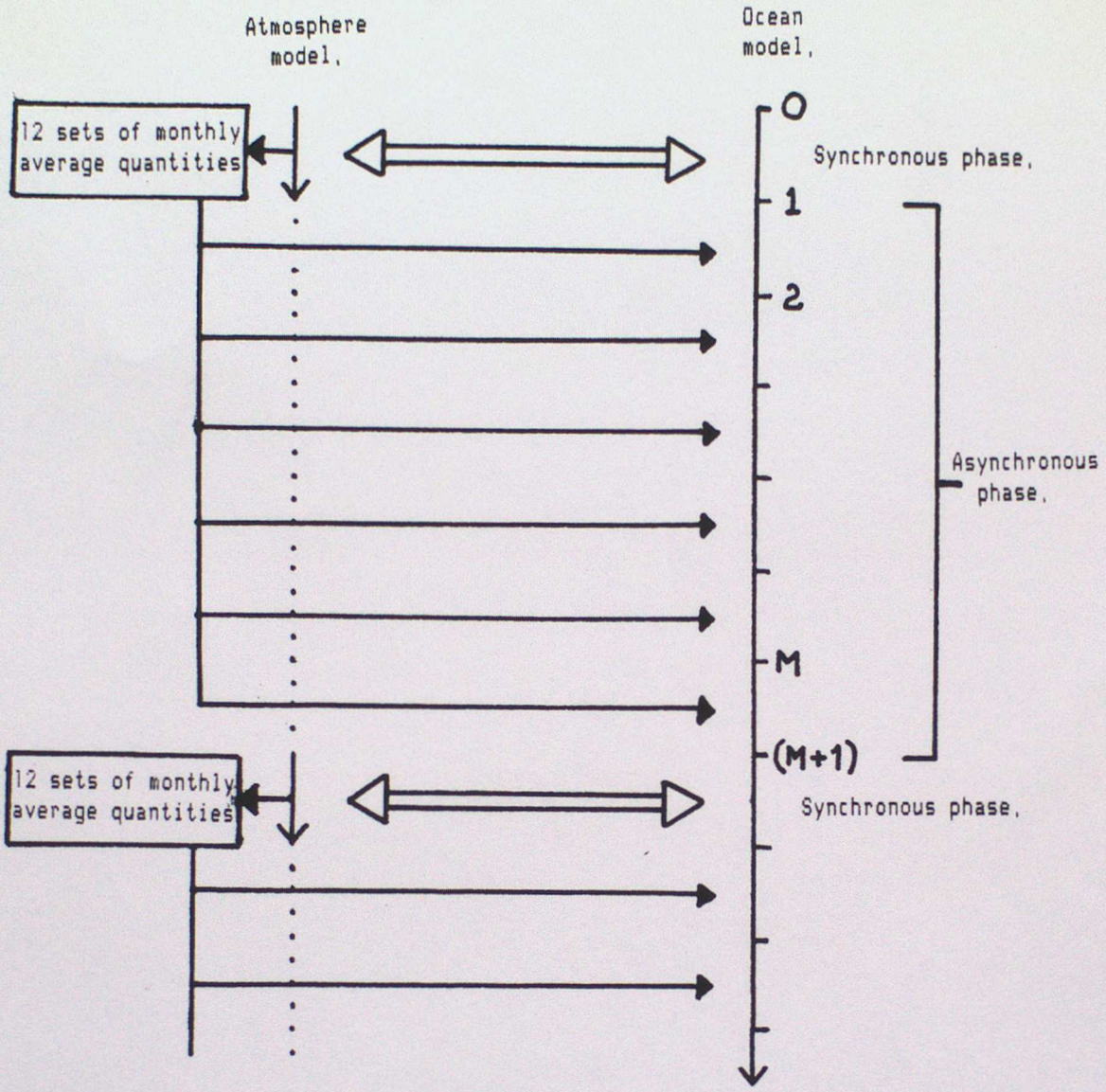

FIGURE 1. The periodically-synchronous coupling scheme due to W.L.Gates. Time in years is marked on the ocean model timeline. The broken line represents periods when the atmospheric model is inactive.

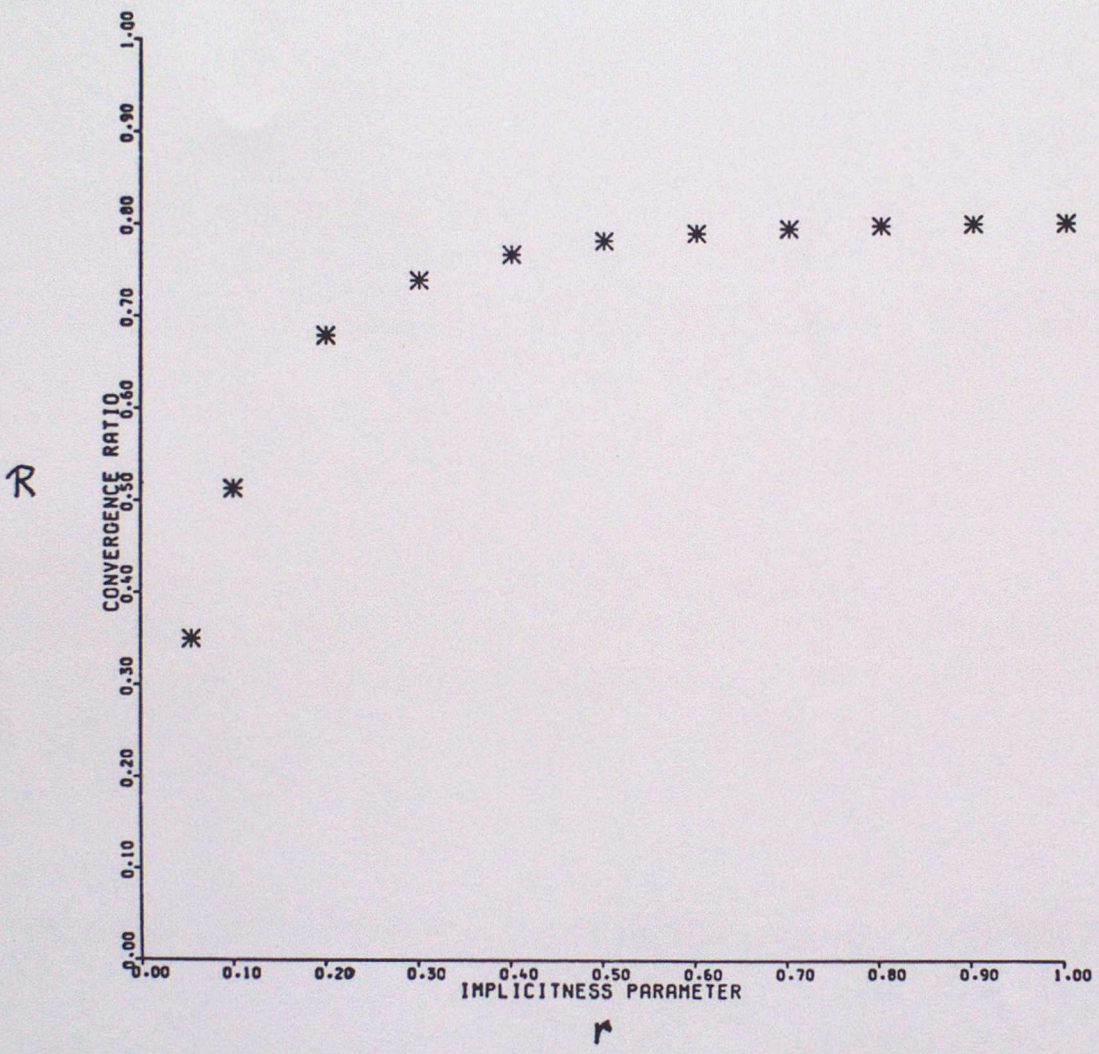

FIGURE 2. Convergence ratios obtained with various values of the implicitness parameter (r), for the two box model with constant perturbation forcing.

FIGURE 3. Evolution of the normalised mixed layer temperature in response to a constant forcing,for the standard three box model. The top curve is the synchronous solution,while the others are asynchronous solutions for (starting with the lowest curve and ascending) r = 1,0.75,0.5,0.25,0.2,0.15,0.1,and 0.05.

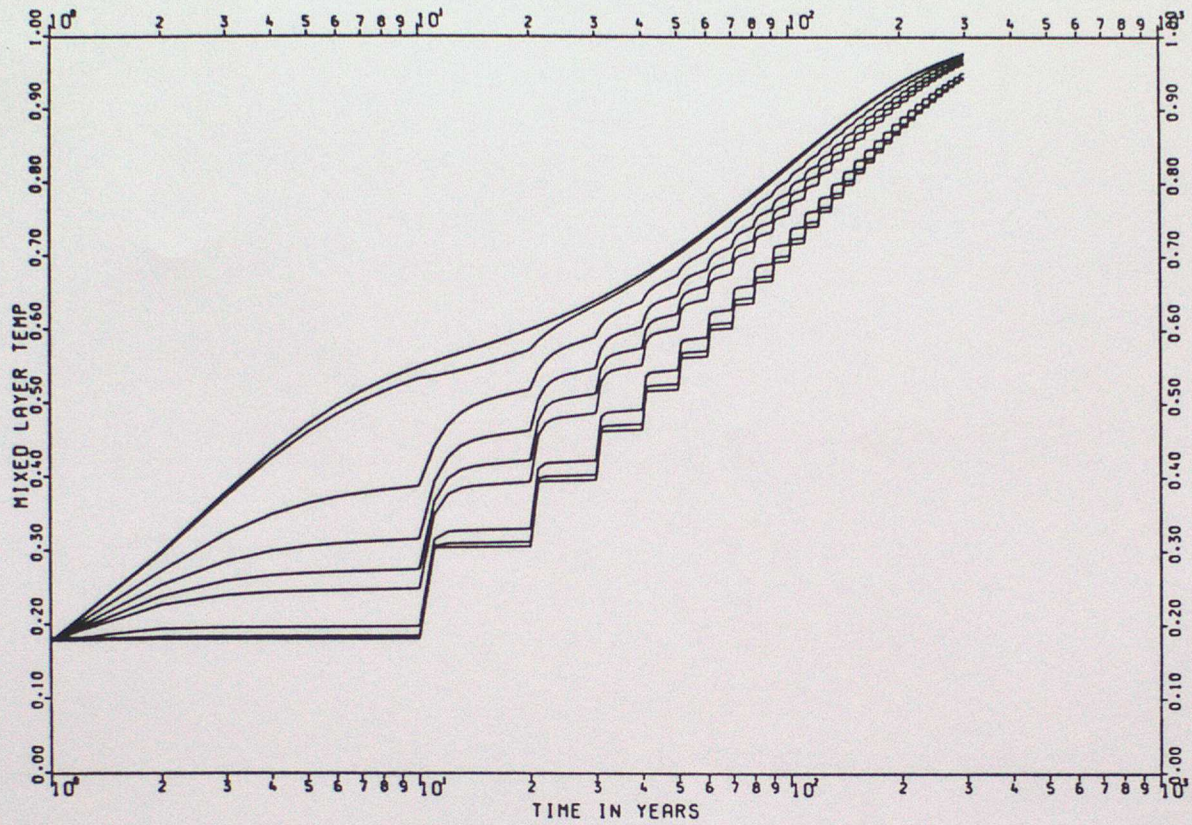

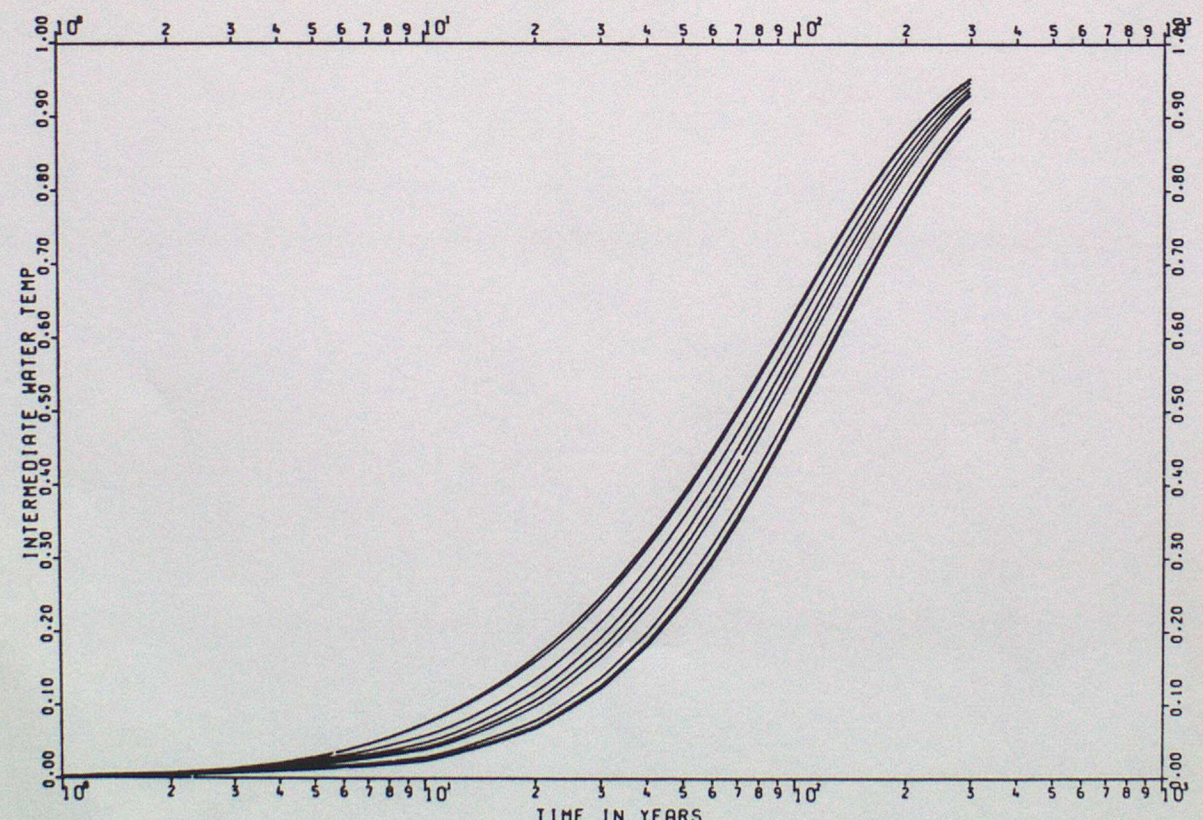

FIGURE 4. Evolution of the normalised deeper water temperature in the same cases as in Figure 3.

FIGURE 5. Evolution of the normalised mixed layer temperature, in cases analogous to those shown in Figure 3,but with λ_{m_o}= 8.

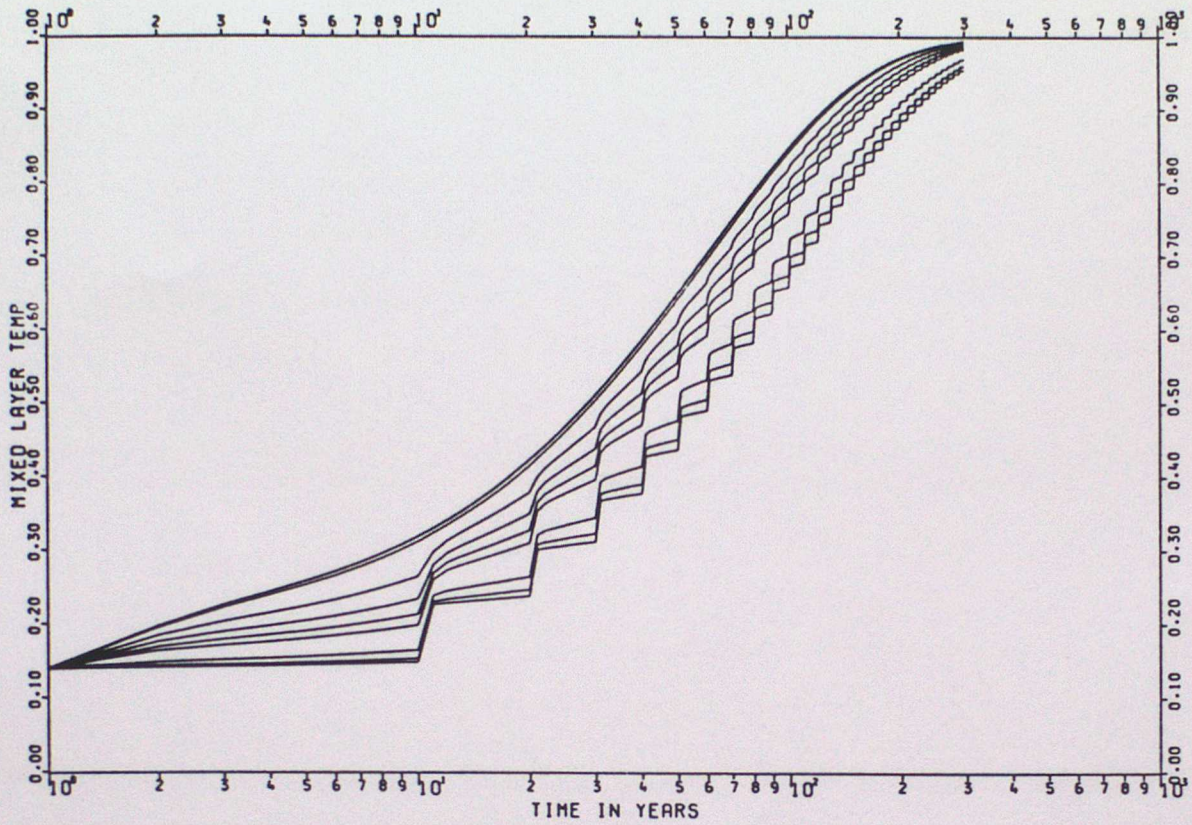

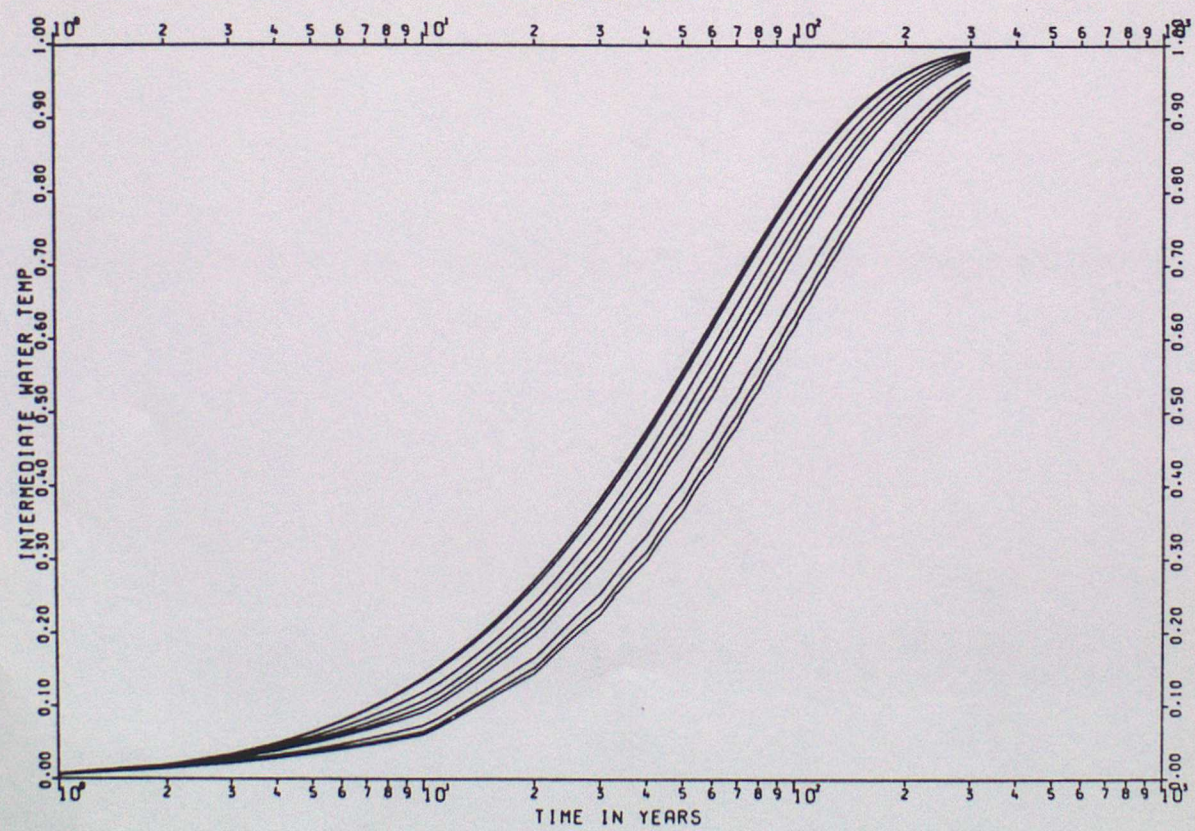

FIGURE 6. Evolution of the normalised deeper water temperature, in cases analogous to those shown in Figure 4,but with λ_{m_o}= 8.

FIGURE 7. Evolution of the normalised mixed layer temperature, in cases analogous to those shown in Figure 3,but with $\lambda_{m\infty}$= 0.5.

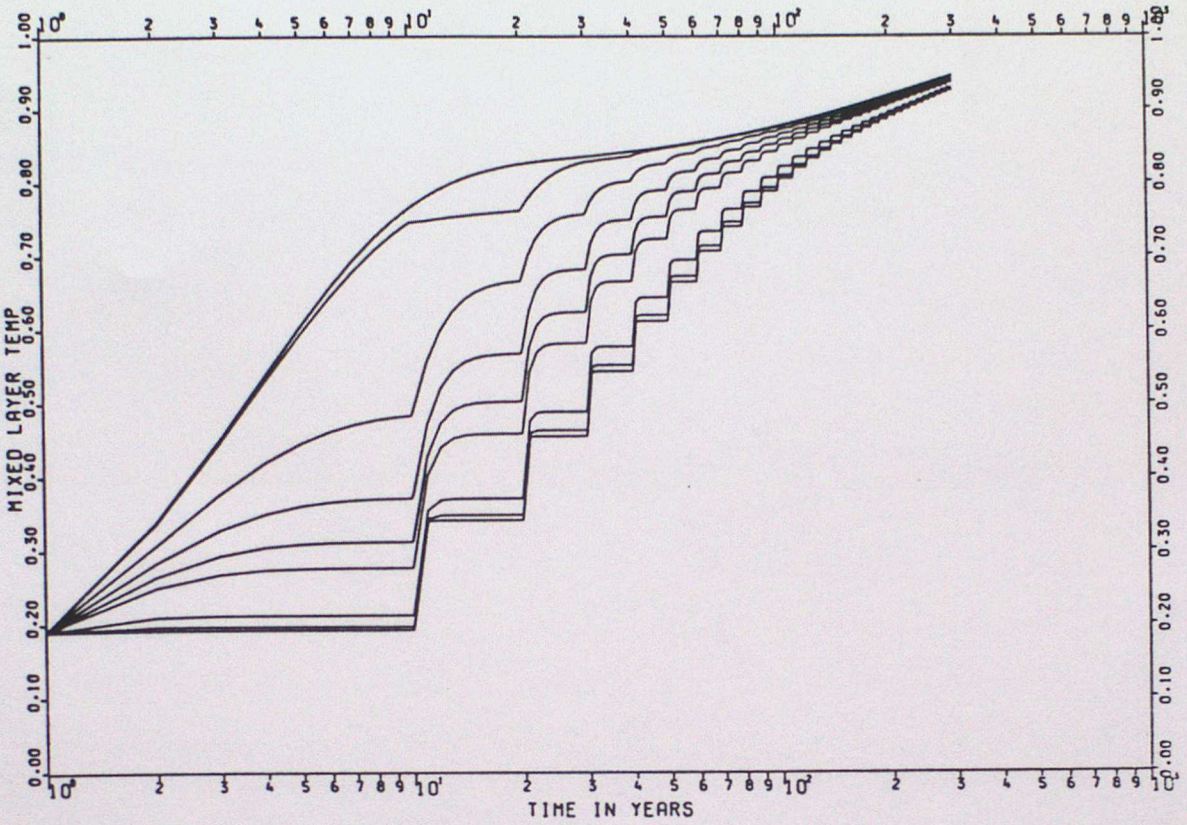

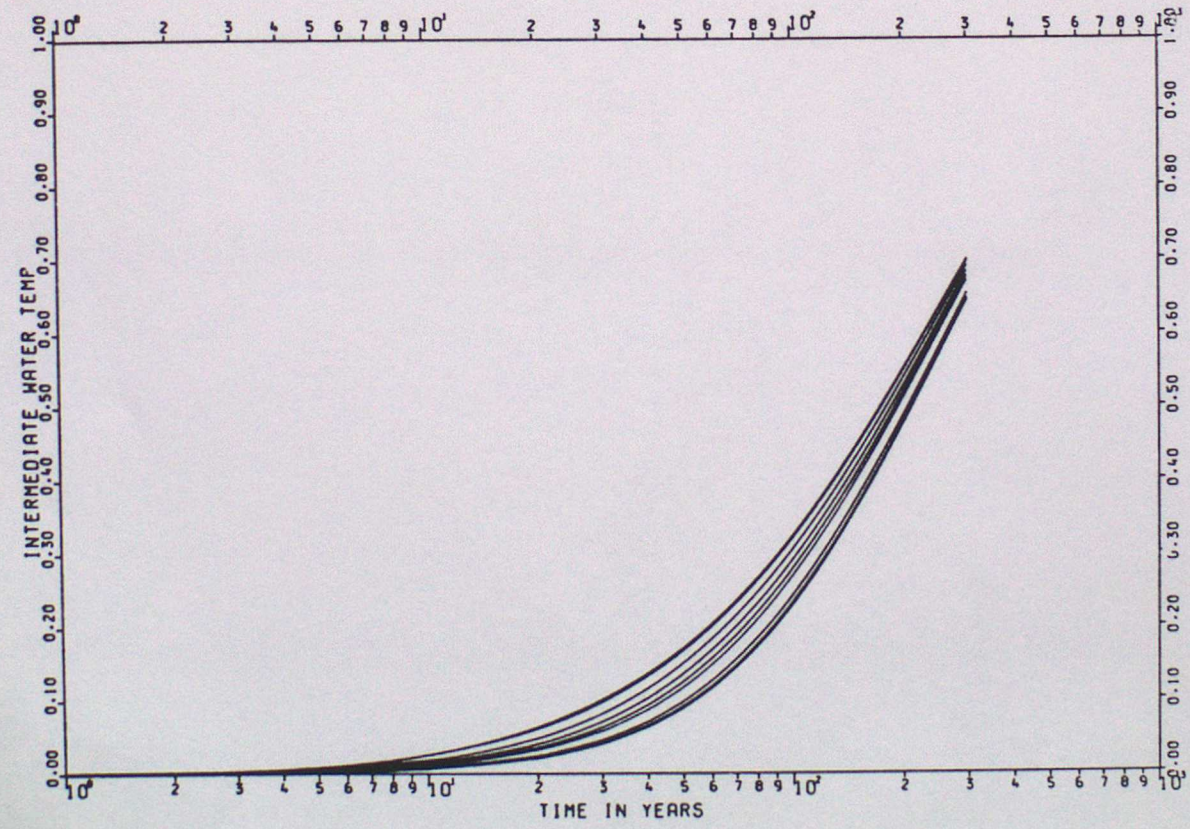

FIGURE 8. Evolution of the normalised deeper water temperature, in cases analogous to those shown in Figure 4,but with $\lambda_{m\infty}$= 0.5.

FIGURE 9. Evolution of the normalised mixed layer temperature in response to a constant forcing,for the standard three box model. The smooth curve is the synchronous solution;the sawtooth curve is the explicit asynchronous solution (i.e. r = 0).

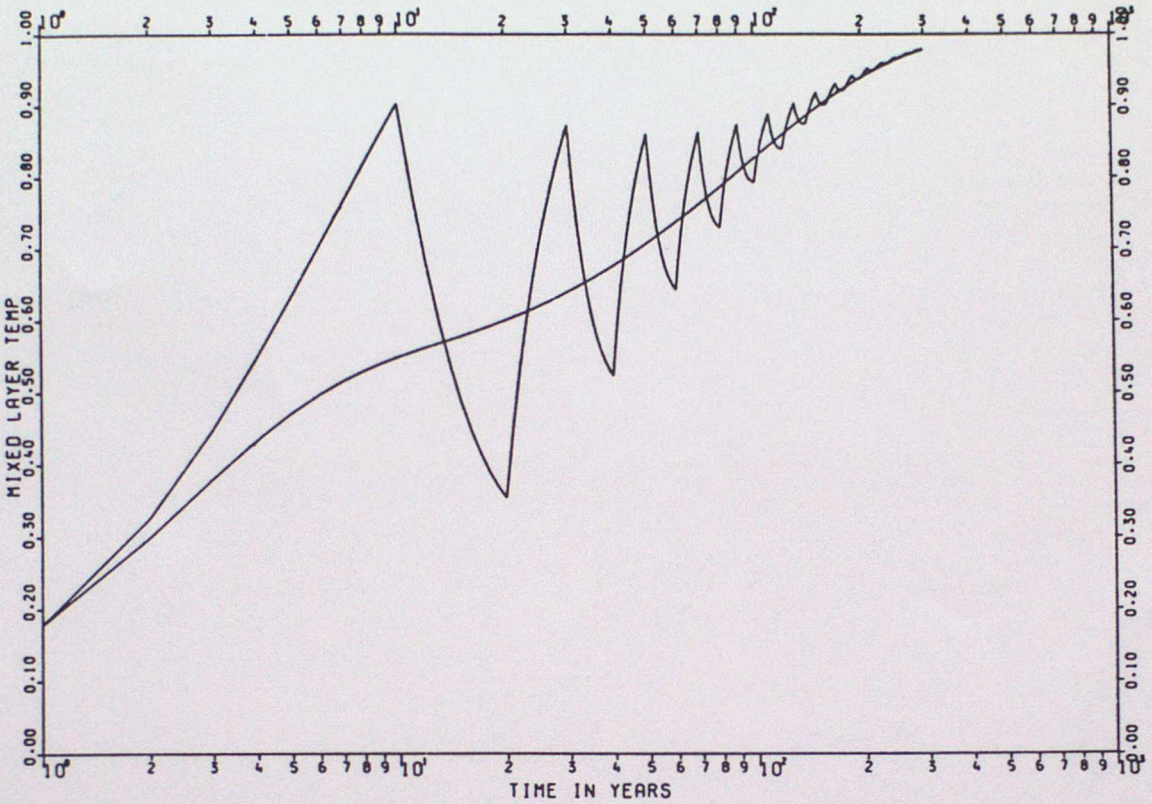

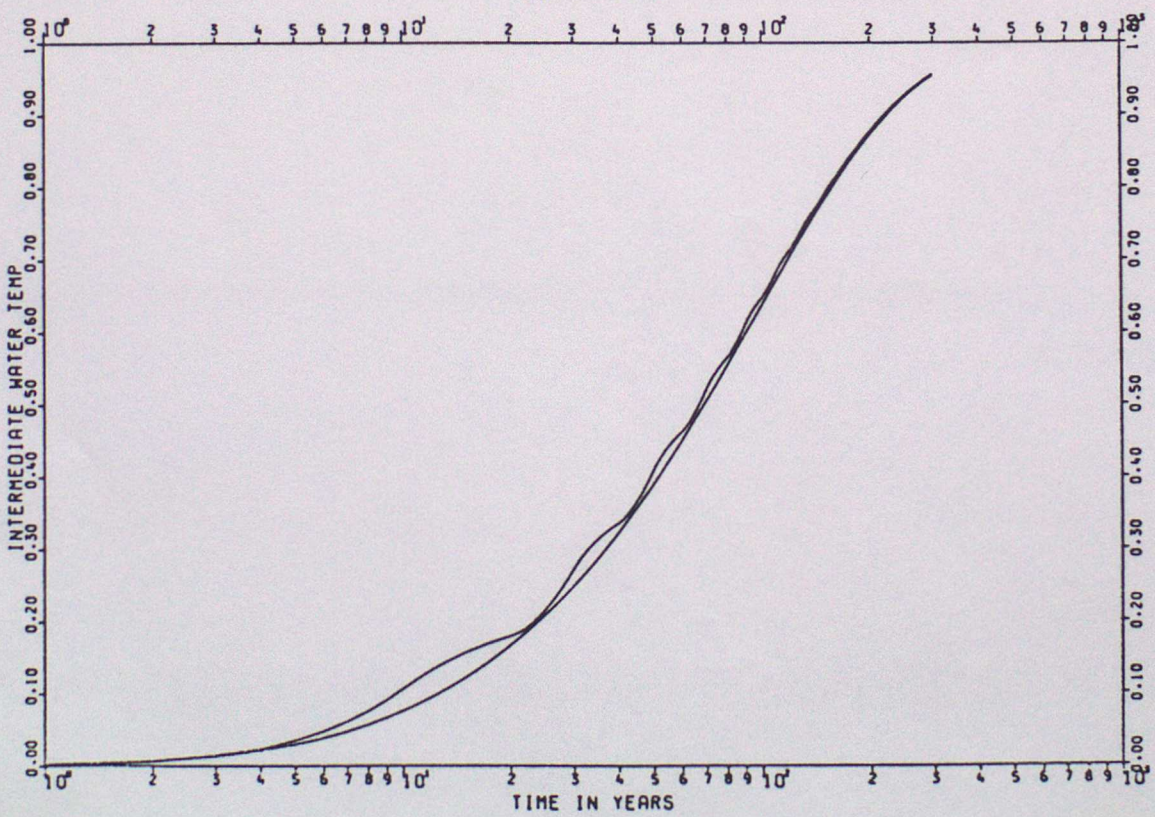

FIGURE 10. Evolution of the normalised deeper water temperature in the cases corresponding to Figure 9.

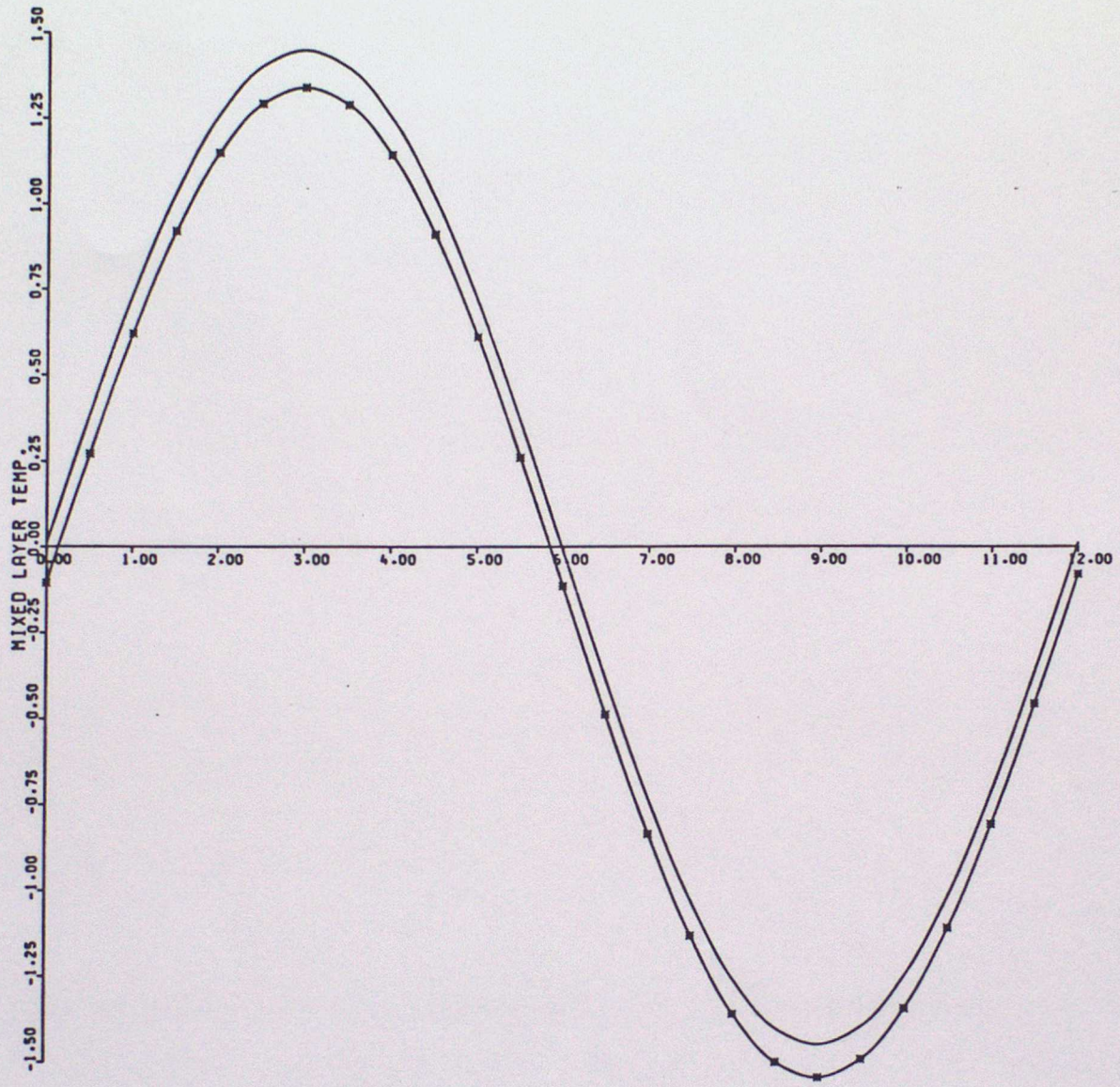

FIGURE 11. Equilibrium response of the (unnormalised) mixed layer temperature to a sinusoidal forcing function,for the standard three box model. The unmarked curve is the synchronous solution,while the marked curve is the annual cycle of the fully implicit asynchronous solution during the synchronous phase. (Here time is in months and (perturbation) temperature in Kelvin.)

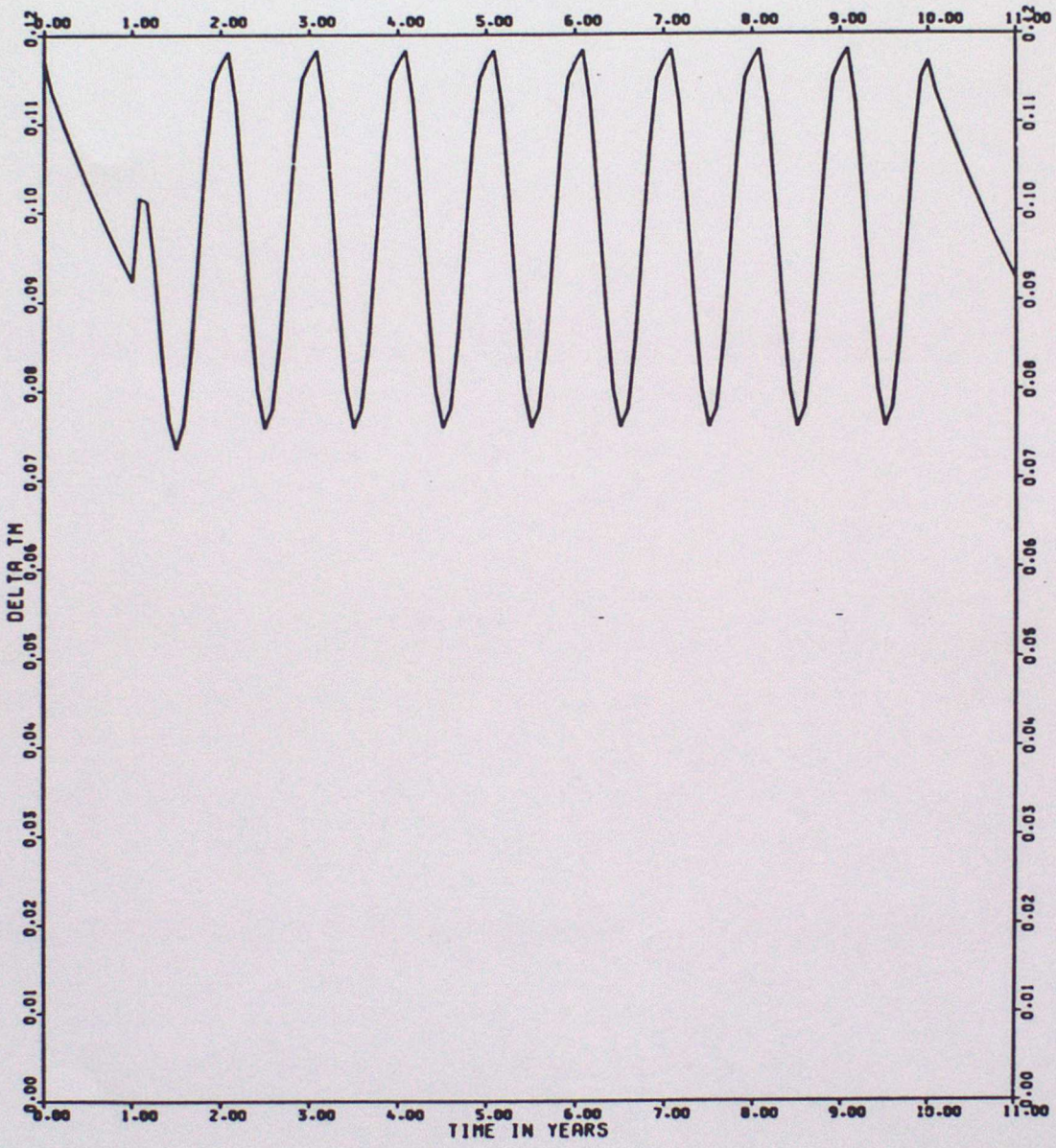

FIGURE 12. The difference between the synchronous and fully implicit asynchronous solutions for the (unnormalised) mixed layer temperature,versus time in years,at equilibrium. The 11 year period begins and ends with a synchronous phase of 1 year.

DYNAMICAL CLIMATOLOGY TECHNICAL NOTES

DCTN 1 June 1984
A scheme for incorporating the thermodynamic sea-ice model into a coupled ocean-atmosphere model.
C Gordon and M Bottomley

DCTN 2 Sept 1984
The parametrization of the upper ocean mixed layer in coupled ocean/atmosphere models.
C Gordon and M Bottomley

DCTN 3 Sept 1984
The response of a simple thermodynamic sea-ice model to GCM forcing appropriate for perennial sea-ice.
M Bottomley

DCTN 4 Sept 1984
Potential vorticity in the stratosphere derived using data from satellites.
S A Clough, N S Grahame and A O'Neill

DCTN 5 Sept 1984
Simulation of the seasonal cycle of SST using globally specified climatological data to force simple ocean models.
N S Grahame

DCTN 6 Sept 1984
Development of an improved GCM radiation scheme.
A Slingo and R C Wilderspin

DCTN 7 Sept 1984
On the specification of surface fluxes in coupled atmosphere/ocean general circulation models.
J F B Mitchell, C A Wilson and C M Price

DCTN 8 Sept 1984
A survey of possible repercussions of the Soviet river reversal programme on Arctic sea-ice.
H Cattle

DCTN 9 Oct 1984
A study of a strong stratospheric warming during January 1982
T D A Fairlie

DCTN 10 Nov 1984
An intercomparison of the Met O 11 M45 model and the Met O 20 11-level model on the Cyber 205
J F Dyson

DCTN 11 Nov 1984
Simulation of observed time series of temperature and precipitation over eastern England.
D N Reed

DCTN 12 Nov 1984
Forecasts and analyses of the onset of the Southwest monsoon.
R Kershaw

DCTN 13 Nov 1984
On modelling the effects of CO_2 on climate.
J F B Mitchell

DCTN 14 Dec 1984
Development of a revised longwave radiation scheme for an atmospheric general circulation model.
A Slingo and R C Wilderspin

DCTN 15 Jan 1985
Rossby wavetrains in the stratosphere forced by localised disturbances in the troposphere.
C J Marks (Oxford), A O'Neill and V D Pope

DYNAMICAL CLIMATOLOGY TECHNICAL NOTES

DCTN 16 Jan 1985
Observing system experiments using the Meteorological Office's 15-level model.
R A Bromley

DCTN 17 Feb 1985
Atmospheric general circulation simulation of the climate of the Mediterranean region.
H Cattle

DCTN 18 Feb 1985
Diurnal variation and cloud in a general circulation model.
C A Wilson and J F B Mitchell

DCTN 19 Feb 1985
The sensitivity of the Saharan region in a general circulation model.
W M Cunnington and P R Rowntree

DCTN 20 Mar 1985
The impact of aircraft observations on analyses and forecasts from the operational 15-level model.
B R Barwell

DCTN 21 Mar 1985
Non-linear effects on heat-induced circulation of the tropical atmosphere.
A E Gill and P J Phlips

DCTN 22 Apr 1985
Simulation of cloudiness with the U.K. Meteorological Office 11-layer AGCM.
A Slingo and R C Wilderspin

DCTN 23 Apr 1985
An integrated approach to the representation of cloud processes. R N B Smith

DCTN 24 May 1985
Nuclear Winter: Calculations of the shortwave radiative effects of soot aerosols.
A Slingo and P Goldsmith

DCTN 25 Jul 1985
Sea ice and the Antarctic winter circulation: a numerical experiment.
J F B Mitchell and T S Hills

DCTN 26 Jul 1985
A Budyko-Sellers model for study of ocean-atmosphere interaction.
W J Ingram

DCTN 27 Aug 1985
The effect of a shoaling thermocline on equatorially-trapped Kelvin waves.
A E Gill and B A King

DCTN 28 Sept 1985
CO_2 climate sensitivity and model dependence of results.
J F B Mitchell, C A Wilson and W M Cunnington

DCTN 29 Sept 1985
Handbook of the Meteorological Office 11-layer atmospheric general circulation model.
Volume 1 : Model Description
Edited by A Slingo

DCTN 30 Sept 1985
Impact of land surface variations on African rainfall in general circulation models.
P R Rowntree, M F Wilson and A B Sangster

DYNAMICAL CLIMATOLOGY TECHNICAL NOTES

DCTN 31 Nov 1985 — The annual cycle of sea level in the eastern tropical Pacific.
G R Bigg and A E Gill

DCTN 32 Nov 1985 — An analytic model of the heat-induced tropical circulation in the presence of a mean wind.
P J Phlips and A E Gill

DCTN 33 Nov 1985 — The effect of resolution and diffusion on the simulated climate.
J F Dyson

DCTN 34 Jan 1986 — Rossby adjustment over a step.
M K Davey, A E Gill, E R Johnson and P F Linden

DCTN 35 Jan 1986 — Issues concerning the evaluation of effective surface roughness of heterogeneous terrain.
D J Carson

DCTN 36 Mar 1986 — Climate sensitivity and past climates : evidence from numerical studies
J F B Mitchell

DCTN 37 Mar 1986 — Parametrisations of land-surface processes in Meteorological Office numerical weather prediction and climate models
D J Carson

DCTN 38 Apr 1986 — Modelling of land-surface processes and their influence on European Climate
D A Warrilow, A B Sangster and A Slingo

DCTN 39 Apr 1986 — Simulation of climatic change due to increased CO_2
J F B Mitchell

DCTN 40 May 1986 — On the interpretation of the Eliassen-Palm flux divergence.
Part I : Theory
D G Andrews

DCTN 41 June 1986 — Experiments on tropical circulation with a simple moist model.
M K Davey and A E Gill

DCTN 42 Jun 1986 — Parameter regimes for studying isolated eddies.
P D Killworth and M K Davey

DCTN 43 Jun 1986 — A comparison of the impact of an envelope orography and of a parametrization of orographic gravity-wave drag on model simulations.
A Slingo and D W Pearson

DCTN 44 Jul 1986 — The effect of a sea-surface temperature anomaly on a prediction of the onset of the south-west monsoon over India.
R Kershaw

DCTN 45 Jul 1986 — An introduction to the parametrization of land-surface processes.
D J Carson

DYNAMICAL CLIMATOLOGY TECHNICAL NOTES

DCTN 46 Sept 1986 — Lateral boundaries and the heat-induced flow in the tropical atmosphere.
P J Phlips and A E Gill

DCTN 47 Nov 1986 — Simulation of the diurnal cycle of outgoing longwave radiation with an atmospheric GCM.
A Slingo, R C Wilderspin and S J Brentnall

DCTN 48 Feb 1987 — A 2 x CO_2 climate sensitivity experiment with a global climate model including a simple ocean
C A Wilson and J F B Mitchell

DCTN 49 Feb 1987 — Sensitivity of the Met O 20 11-layer model to increased land surface roughness length
C C Heasman

DCTN 50 Feb 1987 — The influence of atmospheric waves on the general circulation of the middle atmosphere
D G Andrews

DCTN 51 Feb 1987 — Transport mechanisms in the middle atmosphere: an introductory survey
D G Andrews

DCTN 52 Mar 1987 — The Met O 20 stratosphere-mesosphere model
M Fisher

DCTN 53 Apr 1987 — Simulations of linear and nonlinear disturbances in the stratosphere
A O'Neill and V D Pope

DCTN 54 Apr 1987 — Aspects of dynamics of the middle atmosphere inferred using data from a satellite and from a numerical model
T D A Fairlie and A O'Neill

DCTN 55 Apr 1987 — The seasonal evolution of the stratosphere in the northern hemisphere
A O'Neill and V D Pope

DCTN 56 Apr 1987 — The adjustment of numerical weather prediction models to local perturbations
B R Barwell and R A Bromley

DCTN 57 Jun 1987 — Climate simulations for 9000 years before present: Seasonal variations and the effect of the Laurentide ice sheet
J F B Mitchell, N S Grahame and K J Needham

DCTN 58 Aug 1987 — Climatic effects of nuclear war: the role of atmospheric stability and ground heat fluxes.
J F B Mitchell and A Slingo

DCTN 59 Oct 1987 — The stratospheric major warming of winter 1984/85: observations and dynamical inferences.
T D A Fairlie and A O'Neill

DCTN 60 Oct 1987 — Some comparisons between the middle atmosphere dynamics of the southern and northern hemispheres
D G Andrews

DYNAMICAL CLIMATOLOGY TECHNICAL NOTES

DCTN 61 Jan 1988 Early winter in the northern stratosphere.
M N Juckes and A O'Neill

DCTN 62 Feb 1988 Single column model tests of the Rowntree convection scheme using GATE data.
D Gregory

DCTN 63 Mar 1988 The antarctic winter; simulations with climatological and reduced sea-ice extents.
J F B Mitchell and C A Senior

DCTN 64 Mar 1988 An investigation of the Gates asynchronous coupling strategy using a simple energy-balance model.
D L Roberts